two d electrons per formula unit, and these electrons are primarily confined in the Mo_6O_{22} layers. Thus, only the bottom three of the t_{2g}-block bands of the Mo_6O_{22} layer are partially filled. Our orbital interaction analysis shows that the three partially filled bands are close in energy at Γ, because this wave vector prevents the bridging oxygen p orbitals from mixing with the metal d orbitals. The Fermi surfaces associated with the partially filled bands are all closed, in agreement with the observation that Mo_4O_{11} is a 2D metal. However, the Fermi surfaces show a partial nesting, which is consistent with the superlattice spots at (0, 0.23*b**, 0) found for η-Mo_4O_{11}. The resistivity anomaly in γ- and η-Mo_4O_{11} is most likely to originate from a CDW associated with this partial nesting.

Acknowledgment. M.-H.W. and E.C. thank Dr. J. P. Pouget for invaluable discussions concerning the Fermi surfaces of Mo_4O_{11}. This work was supported by NATO, Scientific Affairs Division, and also by DOE, Office of Basic Sciences, Division of Materials Science, under Grant DE-FG05-86ER45259.

Registry No. Mo_4O_{11}, 12033-38-4.

Contribution from The Frank J. Seiler Research Laboratory, U.S. Air Force Academy, Colorado Springs, Colorado 80840

Calculation of Hydrogen-Bonding Interactions between Ions in Room-Temperature Molten Salts

Chester J. Dymek, Jr.,* and James J. P. Stewart

Received April 26, 1988

The nature of the interactions between the ions in room-temperature molten salts formed by mixing $AlCl_3$ with 1-methyl-3-ethylimidazolium chloride ((MEI)Cl) is of interest because of its relevance to the transport and electrochemical properties of these melts. The results of AM1 semiempirical molecular orbital calculations using the MOPAC program support the interpretation of experimental results in which MEI^+ is hydrogen-bonded to Cl^- ions at the 2-, 4-, and 5-carbons of the MEI^+ ring. A new approach to the characterization of vibrational modes calculated in MOPAC is introduced to more clearly relate the calculated vibrations in the proposed model to experimental results.

Mixtures of 1-methyl-3-ethylimidazolium chloride ((MEI)Cl) and $AlCl_3$ form chloroaluminate salts that are liquid well below room temperature.[1] These melts are of interest as electrolytes, as nonaqueous solvents for studying ionic complexes, and as catalytic solvents for Friedel-Crafts reactions.[2]

The main reactions that occur in the formation of the melts and that explain their interesting acid-base behavior are given as follows:

$$MEI^+Cl + AlCl_3 \rightarrow MEI^+AlCl_4^- \quad K \gg 1$$

$$MEI^+AlCl_4^- + AlCl_3 \rightarrow MEI^+Al_2Cl_7^- \quad K \gg 1$$

Melts formed with mole fraction N of $AlCl_3$ less than 0.5 will have $AlCl_4^-$ and Cl^-, a Lewis base, present and are thus basic melts. Those with $N > 0.5$ contain $AlCl_4^-$ and $Al_2Cl_7^-$, a Lewis acid, and are thus acidic melts. The structure of MEI^+ with ring carbons numbered is shown as follows:

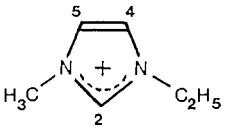

MEI^+

An important aspect of the melts that needs to be further understood is the nature of the interactions among the ions present. The questions of particular interest are the following. Is there ion-pair formation in the melt? Are there specific points on the MEI^+ at which interactions with counterions, particularly Cl^-, occur? Can the transport properties of the melts be understood in terms of these interactions?

NMR[3] and IR[4,5] studies on (MEI)Cl/$AlCl_3$ melts and crystallographic studies[6] of solid (MEI)Cl have been used to propose models for the ionic interactions in the melt. The main differentiation in the models is whether hydrogen bonding occurs between the Cl^- ions and the ring carbons of MEI^+. In a study that presented evidence against hydrogen bonding to Cl^- solely at the C2 hydrogen of MEI^+,[5] a stack model of melt ionic interactions was proposed to explain IR spectral evidence that showed that all three C-H stretches were affected by the presence of Cl^- in basic melts. In this model a Cl^- was sandwiched between two parallel MEI^+ ions that in turn had $AlCl_4^-$ ions on their outer sides. Semiempirical molecular orbital calculations predicted this stack cluster to be stable when fully optimized with the Cl^- approximately centered between the C2's of the two parallel MEI^+ rings. Uncertainty in the validity of this model stemmed from its failure to predict the shift to lower frequencies and the increase in intensity of the C-H stretches experimentally observed with addition of Cl^-. In fact, the ring C-H stretch frequencies differed only slightly from those calculated for an isolated MEI^+. However, attempts to calculate a stable optimized system in which Cl^- is hydrogen-bonded to MEI^+ through the ring C2-H bond also failed. The Cl^- either bonded covalently to C2 of the ring or, if constrained to line up along the C2-H bond, formed virtually a covalent bond with the H. It was acknowledged that these results could not be used to rule out hydrogen bonding of Cl^- to MEI^+ because of the known exaggeration of the instability of Cl^- in the computational method used.

In this work we used the MOPAC program[7] to calculate the optimized molecular structure of MEI^+ in varying ionic environments and then the IR spectra of these optimized systems. We then compared our results with experimental evidence to arrive at a description of the dominant features of the interaction of MEI^+ with Cl^- ions in basic melts.

Computational Methods

The MOPAC program, which incorporates the MNDO,[8] AM1,[9] and MINDO/3[10] semiempirical molecular orbital methods originally developed by Dewar and co-workers, has been applied with some success to

(1) Fannin, A. A., Jr.; Floreani, D. A.; King, L. A.; Landers, J. S.; Piersma, B. J.; Stech, D. J.; Vaughn, R. L.; Wilkes, J. S.; Williams, J. L. *J. Phys. Chem.* **1984**, *88*, 2614.
(2) Hussey, C. L. *Advances in Molten Salt Chemistry*; Mamantov, G., Mamantov, C., Eds.; Elsevier: New York, 1983; Vol. 15, p 185.
(3) Fannin, A. A., Jr.; King, L. A.; Levisky, J. A.; Wilkes, J. S. *J. Phys. Chem.* **1984**, *88*, 2609.
(4) Tait, S.; Osteryoung, R. A. *Inorg. Chem.* **1984**, *23*, 4352.
(5) Dieter, K. M.; Dymek, C. J., Jr.; Heimer, N. D.; Rovang, J. W.; Wilkes, J. S. *J. Am. Chem. Soc.* **1988**, *110*, 2722.
(6) Dymek, C. J., Jr.; Fratini, A. V.; Adams, W. W.; Grossie, D. A. *Inorg. Chem.*, in press.
(7) Stewart, J. J. P. *Quantum Chem. Prog. Exchange Bull.* **1987**, *7(4)*, addendum.
(8) Dewar, M. J. S.; Thiel, W. *J. Am. Chem. Soc.* **1977**, *99*, 4899.
(9) Dewar, M. J. S.; Zoebisch, E. G.; Healy, E. F.; Stewart, J. J. P. *J. Am. Chem. Soc.* **1985**, *107*, 392.
(10) Bingham, R. C.; Dewar, M. J. S.; Lo, D. H. *J. Am. Chem. Soc.* **1975**, *97*, 1285.

Table I. MOPAC-Generated Description of the C–I Stretching Mode in Iodomethane

vibration no.	1	travel, Å	0.689
freq, cm^{-1}	721.48	red mass, amu	9.8343
transn dipole, D	0.6929		

atom pair	% energy contrbn	% radial comp	atom pair	% energy contrbn	% radial comp
I1---C2	30.7 (121.6)	100.0	C2---H4	23.1	11.8
C2---H5	23.1	11.8	C2---H3	23.1	11.8

liquid ionic systems.[11,12] Calculations on molecular ions in ionic liquids have predicted or supported experimental results through the use of clusters of ions, surrounding the molecular ion of interest, to simulate the condensed-phase environment. Briefly, in this computation technique, the user defines the internal coordinates of the system of interest. MOPAC then calculates the system geometry that has the minimum heat of formation. Other system properties, such as charge distribution, dipoles, and vibrational frequencies, can then be obtained for this optimized geometry. In the calculations reported here, the AM1 method[9] was used. The overall operation of MOPAC has been described in some detail.[7] We next describe a new approach that we incorporated into the MOPAC program and used in the normal-coordinate analysis and characterization of the normal models in this work.

Normal-Coordinate Analysis

Normal modes are of limited use of assigning the relative importance of each atom in a given vibration. Thus, for example, in iodomethane it is not obvious from an examination of the normal modes which mode represents the C–I stretch. A more useful description is provided by the energy, or mass-weighted, coordinate analysis, the results of which are shown in Table I. Within iodomethane the C–I vibration has the lowest frequency, 721.48 cm^{-1}, a transition dipole of 0.6929, and a reduced mass of 9.8343 amu. If the vibration is assumed to be simple harmonic, then it can be represented by a finite mass (the reduced mass) connected by a spring to an infinite mass, the finite mass oscillating through a distance of 0.0689 Å.

Relative motion of two atoms can be partitioned into radial and tangential components. The radial component of relative motion is presented in the last column of Table I. The C–I mode shown in Table I transforms as A under the C_{3v} point group and thus is 100% radial. The major difference in the Table I output from previous MOPAC vibrational analyses involves the energy contribution column.

In this analysis, the energy absorbed by each atom (E_{AA}, E_{BB}, ...) and the energy absorbed or released by each bond (E_{AB}, E_{BC}, ...) is calculated for each vibrational model. Two atoms are considered as bonded if their interatomic distance is within 1.5 times the sum of their covalent radii. In a given mode, the energy change associated with an atom, E_{AA}, is calculated from its displacement and the force resisting the displacement (the force constants), and thus $E_{AA} \geq 0$. [Strictly, we use the atom's instantaneous velocity vector, the x, y, and z components of which describe the motion of the atom relative to the system center of gravity. This is obtained by diagonalizing the mass-weighted Hessian matrix (formed from the second derivatives of the heat of formation of the system) with respect to the Cartesian coordinates.] The energy change associated with the A–B bond, E_{AB}, is calculated from the simultaneous relative displacement of atoms A and B and the net resisting force. E_{AB} may be positive or negative. A loose interpretation of this algebraically driven result is that a bond may absorb part of the energy of the photon stimulating the mode or it may release energy to the other motions in the mode. In any case, the energy of a given pair of atoms is calculated as

$$E(\text{A–B}) = E_{AA} + E_{BB} + 2E_{AB}$$

The total energy of all the pairs of bonded atoms in the molecule in the mode is then given by

$$E_{tot} = \sum_{A}\sum_{B} E(\text{A–B})$$

The output that the MOPAC program generates as the description of vibrations gives the energy contribution for each bonded pair as the percentage, $[E(\text{A–B})/E_{tot}] \times 100$. Thus, in Table I it can be seen that in the first mode of vibration of CH_3I, the C–I pair, with 30.7% energy contribution, is where the energy is concentrated. Note however that the contribution from the C–H pairs is only slightly lower at 23.1%. The assignment of this mode as a C–I stretch is emphasized by including in parentheses after the C–I contribution the "absolute contribution" (121.6%). This is the energy of the C–I pair, E(C–I), divided by the energy of the stimulating photon, $h\nu$. That E(C–I) is greater than $h\nu$ stems from the fact, which is not presented as output, that the E_{CI} term is positive (the C–I bond absorbs energy) while the E_{CH} terms are negative (the C–H bonds release energy in the mode). From this analysis, we conclude that the mode is indeed the C–I stretch.

Interpretation of this new MOPAC output requires an understanding that E_{tot} is greater than $h\nu$ because multiple counting of atom-displacement energies occurs. For example, note that in the CH_3I mode described, E_{CC} is included in E(C–I) as well as in the three E(C–H) energies. It can be concluded from this that the carbon atom is the one whose energy is most increased by the stimulating photon. Further, assignment of the mode to a particular motion, in this case, the C–I stretching motion, is based on which atom pair has the highest "absolute contribution", indicating that this particular bond (or bonds) absorbs more of the stimulating photon's energy than other bonds. Finally, highest absolute contributions exceedng 100% indicate that negative contributions, i.e., energy release, must occur in other bonds in the molecule.

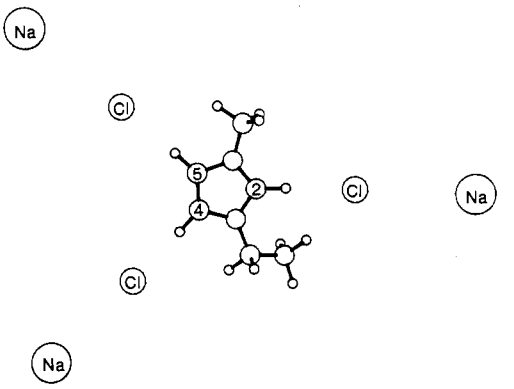

Figure 1. Optimized geometry from AM1 calculation on MEI^+ with ring H---Cl^- distances fixed at 2.6 Å, Cl^----Na^+ distances fixed at 4.5 Å, and ring C–H---Cl^- and ring C–H---Na^+ angles fixed at 178°.

Results and Discussion

Crystallographic evidence[6] has shown that in (MEI)Cl crystals, each MEI^+ has three Cl^- ions as nearest neighbors in positions nearly along the lines of the ring C–H bonds (C–H---Cl^- angles of 138–167°) and at distances close to what would be considered hydrogen-bond distances (ring C–Cl^- distance from 3.4 to 3.7 Å). This prompted us to perform further calculations of $MEI^+ + Cl^-$ systems in which Cl^- is constrained to fixed distances nearly along the lines of the ring C–H bonds. To balance the charge of the Cl^- ions in these positions, simulated Na^+ ions (called "sparkles" in MOPAC) were positioned on the side of each Cl^- opposite from the MEI^+. This system is shown in Figure 1.

A series of calculations were done on this system in which the ring C–H---Cl^- angles were fixed at 178°, the Na^+–Cl^- distances and ring C–Cl^-–Na^+ angles were fixed at 4.5 Å and 178°, respectively, and the ring H–Cl^- distances were fixed at values ranging from 2.0 to 3.0 Å. The value of 178° for the C–H---Cl^- angle is larger than what occurs in the crystal but may be closer to what would be expected in the liquid, which is our main interest. A C–H---Cl^- angle of 180° was not chosen, as this is a very low probability angle: in a uniform spherical distribution the statistical weight of occurance at the angle t in the region of 180° varies as $(180 - t)^2$. The 4.5-Å distance for Na^+–Cl^- was selected on the basis of the approximate distance from Cl^- to the center of an interacting MEI^+. All atoms in the MEI^+ were allowed to optimize to the most stable configuration. Then MOPAC calculations of the vibrational spectra were done on these optimized systems, with the Na^+ sparkles and Cl^- ions being assigned very large atomic weights to keep them virtually "immobilized" in the normal modes of the system. The frequencies of the ring C–H stretches as a function of the ring H–Cl^- distances are shown in Figure 2. The width of the "Cl^- interaction band"[5] at half its maximum intensity is indicated by the dashed lines in this figure. This band appears in the MEI^+ spectrum with increasing intensity as more Cl^- is present in (MEI)Cl/$AlCl_3$ melts (see Figure 3).

(11) Davis, L. P.; Dymek, C. J., Jr., Stewart, J. J. P.; Clark, H. P.; Lauderdale, W. J. *J. Am. Chem. Soc.* **1985**, *107*, 5041.
(12) Dymek, C. J., Jr.; Einarsrud, M.-A.; Wilkes, J. S.; Oye, H. A. *Polyhedron* **1988**, *7*, 1139.

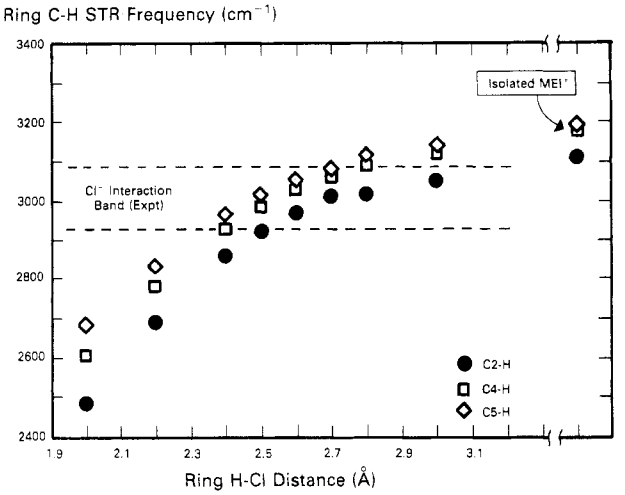

Figure 2. Calculated ring C–H stretching frequencies for MEI^+ as a function of fixed ring C---Cl^- distance in the Figure 1 configuration.

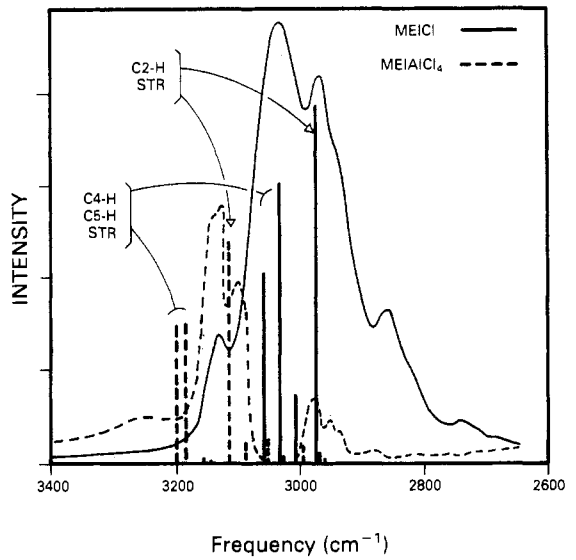

Figure 3. Comparison of experimental[13] and calculated IR spectra of (MEI)Cl and $(MEI)AlCl_4$ in C–H stretching region. MOPAC-generated frequencies are indicated by vertical bars (solid line = Figure 1 configuration; dashed line = isolated MEI^+).

The frequencies calculated from the isolated MEI^+ are also shown on the rightside of Figure 2. On the basis of this figure, the observed shift is most closely modeled with the Cl^- ions between 2.4 and 2.7 Å from the ring H's. This prediction is in good agreement with the ring H–Cl^- distances of 2.3–2.6 Å observed in the (MEI)Cl crystal.[6]

AM1 is the first NDO-type semiempirical method to accurately predict the strength of the hydrogen bond in both neutral[10,13] and charged systems.[14] The principal contributions to the energy in hydrogen bonds in AM1 are due to the spherical Gaussian core–core interactions and dipole–dipole terms. The core–core terms may be regarded as representing the correlation attraction interaction, while the dipole–dipole terms represent the electrostatic contribution. Stabilization due to transfer of electrons or exchange terms is relatively unimportant in neutral systems but can become more important in charged systems.[14] In the case of charged systems of the type described here the stabilization is due primarily to charge–dipole interactions.

While our results support the hydrogen-bonding model, we cannot ignore the possibility that other factors may have influenced the calculated results. For example the Cl^-–Na^+ pairs in the Figure 1 model may have caused the ring C–H stretches to be significantly mixed with other motions of MEI^+. This could result in contaminated modes giving rise to shifted frequencies. In the examination of such possibilities, the simple vector diagrams of the modes are of limited use. Far more convincing evidence that the shift is due to electrostatic interactions between the ring C–H bonds and the Cl^- ions (i.e. hydrogen bonding) would be that the shift occurs even though the distribution of energy within the mode itself remains unchanged. The descriptions of the ring C–H vibrations for the isolated MEI^+ and the Figure 1 configuration are shown in Table II.

The results show that the modes are clearly the ring C–H stretches. We see that virtually all the energy of these modes is carried by the ring hydrogens. The expectation that the C4–H and C5–H bonds are strongly coupled through the C4=C5 double bond is confirmed by the near equality of the energy contributions of the C4–H and C5–H stretches in both systems. Most significantly, the close correspondence of the modes in the two systems confirms that the Figure 1 model resulted in a straightforward calculation, uncomplicated by the presence of the Cl^-–Na^+ pairs

Table II. MOPAC-Generated Description of the Ring C–H Stretching Vibrations in Isolated MEI^+ and Figure 1 Configurations

Isolated MEI

vibration no.	48	travel, Å	0.1176
freq, cm^{-1}	3117.84	red mass, amu	0.7812
transn dipole, D	1.0350		

atom pair	% energy contrbn	% radial comp	atom pair	% energy contrbn	% radial comp
C1---H2	91.4 (99.3)	100.0	C1---N6	1.8	37.1
C1---N3	1.8	37.1	C1---C4	1.8	87.0

vibration no.	50	travel, Å	0.1196
freq, cm^{-1}	3187.64	red mass, amu	0.7389
transn dipole, D	0.8128		

atom pair	% energy contrbn	% radial comp	atom pair	% energy contrbn	% radial comp
C5---H8	48.8 (72.1)	100.0	C4---C5	1.2	0.0
C4---H7	45.4	100.0	C1---C5	0.8	82.7

vibration no.	51	travel, Å	0.1149
freq, cm^{-1}	3200.56	red mass, amu	0.7972
transn dipole, D	0.8044		

atom pair	% energy contrbn	% radial comp	atom pair	% energy contrbn	% radial comp
C4---H7	47.7 (71.5)	100.0	C4---C5	2.0	100.0
C5---H8	44.2	100.0	C1---C4	0.9	90.9

Figure 1 Configuration

vibration no.	60	travel, Å	0.1173
freq, cm^{-1}	2972.32	red mass, amu	0.8244
transn dipole, D	2.0248		

atom pair	% energy contrbn	% radial comp	atom pair	% energy contrbn	% radial comp
C1---H2	85.0 (96.7)	100.0	C1---N3	2.2	41.0
C16---H18	2.7	99.9	C1---N6	2.2	35.2

vibration no.	65	travel, Å	0.1213
freq, cm^{-1}	3032.58	red mass, amu	0.7557
transn dipole, D	1.7600		

atom pair	% energy contrbn	% radial comp	atom pair	% energy contrbn	% radial comp
C5---H8	45.7 (70.1)	100.0	C13---H14	2.4	98.2
C4---H7	43.1	100.0	C13---H15	1.5	94.7

vibration no.	66	travel, Å	0.1140
freq, cm^{-1}	3057.72	red mass, amu	0.8485
transn dipole, D	1.4440		

atom pair	% energy contrbn	% radial comp	atom pair	% energy contrbn	% radial comp
C4---H7	46.2 (70.8)	100.0	C4---C5	2.5	100.0
C5---H8	41.3	100.0	C1---H2	2.3	100.0

(13) AM1 predicts the strength of the hydrogen bond in the water dimer as 5.5 kcal/mol, see: Stewart, J. J. P. *Comput. Chem.* **1989**, *13*, 157. The value given in ref 9, 3.5 kcal/mol, is incorrect.

(14) Galera, S.; Lluch, J. M.; Oliva, A.; Bertran, J. *THEOCHEM* **1988**, *163*, 101.

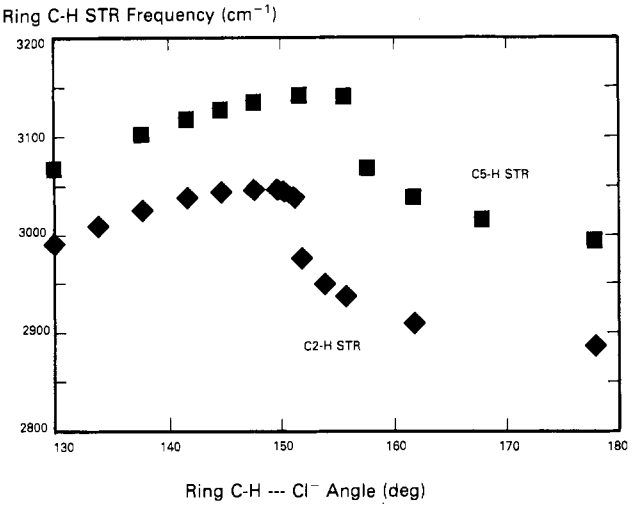

Figure 4. Calculated ring C–H stretching frequencies for MEI^+ interacting with one Cl^----Na^+ pair as a function of the ring C–H---Cl^- angle. (H---Cl^- distance is fixed at 2.6 Å; Na^+---Cl^- distance is fixed at 4.5 Å; C–H---Na^+ angle is fixed at the same angle as the ring C–H---Cl^- angle.)

and the constraints imposed on the system. The observed shift in the frequencies and the change in transition dipoles can therefore be attributed to the interactions of the ring C–H bonds with the Cl^- ions, as expected for hydrogen bonding. Thus, a model in which Cl^- is hydrogen-bonded at C2, C4, and C5 of MEI^+ correctly predicts the shifts in the ring C–H stretching frequencies observed in going from neutral (no Cl^- present) to basic (Cl^- and $AlCl_4^-$ present) melts.[5] A comparison of the calculated and experimental spectra is shown in Figure 3.

In the (MEI)Cl crystal structure, the Cl^- ions are not in all cases on the lines of the ring C–H bonds with which they hydrogen-bond. It was therefore of interest to determine the effect of the ring C–H---Cl^- angle on the C–H stretching frequencies. The H–Cl^- and Na^+–Cl^- distances at the C2 position were fixed at 2.6 and 4.5 Å, respectively. The ring C2–H---Cl^- angles were fixed at values ranging from 130 to 178°. No Cl^-–Na^+ pairs were placed at the C4–H and C5–H positions. A similar series was done on the C5–H---Cl^- angle with the C2–H and C4–H positions free of Cl^-–Na^+ pairs.

A plot of the affected ring C–H stretches as a function of the ring C–H---Cl^- angle is shown in Figure 4. It appears that, above 160°, the frequencies of the ring C–H stretches do not differ significantly from the observed ring C–H stretch frequencies in the Cl^- interaction band. Below 160° the frequencies slowly rise, corresponding to a smaller shift of the Cl^- interaction band. The decrease in frequencies at angles lower than about 150° seems to be due to the close approach to Cl^- to hydrogens on the alkyl groups. At 148°, the Cl^-–alkyl H H distance is 1.970 Å for the Cl^- at the C2–H bond and 1.886 Å for the Cl^- at the C5–H bond. At 178°, these distances are 3.755 and 3.683 Å, respectively. The interaction of Cl^- with the alkyl H's would probably be slightly different if the H---Cl^- distance were not fixed at 2.6 Å. The important result here is that the effect of the C–H---Cl^- angle on the C–H stretching frequencies is consistent with the hydrogen-bonding interpretation of the experimental result.

This calculation also pointed out that the calculated shift in the C–H stretching frequency was somewhat greater when only a single ring C–H is affected than when Cl^- ions are present at all three ring C–H bonds. Table III compares the ring C–H stretching frequencies for the cases with isolated MEI^+, with single Cl^- ions present, and with three Cl^- ions present.

While the results described above support the hydrogen-bonding model for Cl^-–MEI^+ interactions in these melts, the need to constrain the ring H---Cl^- distance keeps the approach from being wholly satisfying. Thus, another set of calculations was done in which, starting with the Figure 1 geometry, we allow the whole system to optimize. The fully optimized geometry is shown in Figure 5. Cl^- at C2 now moves to 1.844 Å from C2–H, resulting

Table III. Calculated C–H Stretching Frequencies

	stretching freq, cm^{-1} (transn dipole, D)		
syst[a]	C2–H	C4–H	C5–H
isolated MEI^+	3117.8 (1.04)	3187.6 (0.81)	3200.6 (0.80)
MEI^+ + 3 Cl^-–Na^+	2972.3 (2.02)	3032.6 (1.78)	3057.7 (1.44)
MEI^+ + 1 Cl^-–Na^+			
at C2	2884.6 (2.37)	3209.2 (0.76)	3221.2 (0.73)
at C4	3143.6 (0.88)	2992.5 (2.09)	3210.8 (0.79)
at C5	3144.8 (0.90)	3210.3 (0.74)	2994.3 (2.09)

[a] Fixed coordinates: ring CH–Cl^- distances all at 2.6 Å; Cl^-–Na^+ distances all at 4.5 Å; ring C–H---Cl^- and ring C–H–Na^+ angles all at 178°.

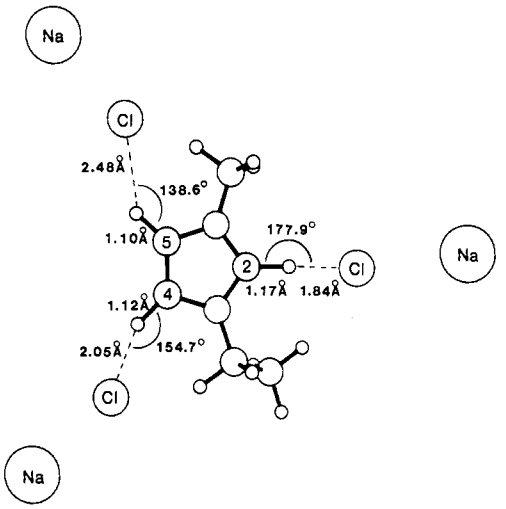

Figure 5. Calculated fully optimized geometry obtained by removing all constraints from Figure 1 geometry.

in a much greater shift (down to 2382.2 cm^{-1}) than is experimentally observed. Further, the mode in which this stretch is dominant is considerably mixed with an H–Cl^- stretch, the energy contributions being 50.1% C2–H and 39.3% H–Cl^-. Thus, when the system is allowed to fully optimize, the Na^+ does not adequately represent the competing pull on the Cl^- of two MEI^+ ions. What may be more revealing about this result are the distances and the angles at which the ring C–H---Cl^-'s optimized. At the C4 and C5 positions, these angles are considerably smaller than 180° and the H---Cl^- distances are somewhat larger. Thus, the shifts in the C–H frequencies are not nearly as large as that which occurred at the C2 position (C4–H at 2828.3 and C5–H at 3123.5 cm^{-1}).

These interaction geometries may be understood by recognizing that the three Cl^- ions surrounding the MEI^+ are forced into a near-equilateral geometry by electrostatic repulsion. MEI^+ finds the most stable position inside this triangle by minimizing the C–H---Cl^- distances at all three ring carbons. Because the ring C–H's form an isosceles triangle, at best only one C–H---Cl^- angle can be at or near 180° (and consequently the minimum H---Cl^- distance). The C–H---Cl^- angles for the other two ring carbons must be less than 180° and must be bent in directions opposite from each other. If they were bent in the same direction, there would be an electrostatic pull in that direction. In the absence of some counter to that force, this would not be an equilibrium position. Since no such counter force appears in this system, that most stable equilibrium arrangement must have the two nonlinear interacting C–H's bent in opposite directions. The only arrangement satisfying this requirement is the one shown in Figure 5.

Another possible contribution to the smaller angles and larger H---Cl^- distances at the C4 and C5 positions is the electrostatic attraction of the Cl^- ions for the hydrogens on the alkyl groups. At the C2 position, this attraction is approximately symmetrical, so the C2–H---Cl^- angle optimized at 177.9°. The Cl^- ions at the 4- and 5-positions will be attracted to acidic H's on the alkyl groups at the adjacent nitrogens. Thus, the geometry of the ring

may be a factor in making C2-H---Cl^- a stronger hydrogen bond than those at the 4- and 5-positions. This difference is most evident in the experimental observation[3] that the NMR shift of the C2 proton changes more rapidly with Cl^- concentration than do the NMR shifts of the C4 and C5 protons.[3]

Another factor that must be considered in explaining the NMR results is the relative acidity of the three ring H's. In the isolated MEI^+, the C2 hydrogen is predicted by AM1 to have a +0.25 charge while the C4 and C5 hydrogens have +0.23 charges. While this difference is almost insignificant, it is at least in qualitative agreement with the observation that isotopic exchange of ring hydrogens with deuterium occurs more readily at the C2 position for MEI^+ in D_2O.[15]

While the computational results described above give some insight into the structural causes of the experimental results, it must be kept in mind that predicting the shifted frequencies could only be accomplished by constraining the ring H-Cl^- distances. This required constraint may seem to be a flaw in the model. However, it is reasonable to argue that such constraints are needed when it is desired to simulate the condensed phase with gas-phase clusters. In the condensed phase, the Cl^- ions are constrained from approaching closer to the ring C-H's by the pull of surrounding MEI^+ ions. The competing positive charges simulated by the Na^+ sparkles are constrained from closer approach to the central MEI^+ by the pull of surrounding anions as well as electrostatic repulsion and steric effects.

(15) Wilkes, J. S., The Frank J. Seiler Research Laboratory, U.S. Air Force Academy, Colorado Springs, CO 80840. Unpublished result.

Conclusions

Semiempirical molecular orbital calculations using the MOPAC program have correctly predicted the shifts in ring C-H stretching frequencies observed for MEI^+ due to interaction with Cl^- counterions. The interaction can best be classified as hydrogen bonding of Cl^- at the three ring C-H positions. The stronger interaction observed at the C2-H position (on the basis of proton NMR shift dependence on Cl^- concentration) can likely be attributed to structural factors involving the two alkyl groups and, more significantly, the nonequilateral triangular shape of the three ring C-H positions. These factors allow Cl^- to interact with C2-H at a C2-H---Cl^- angle approaching 180° while influencing the C4-H---Cl^- and C5-H---Cl^- angles to optimize at smaller angles and larger H---Cl^- distances.

Registry No. $AlCl_3$, 7446-70-0; 1-methyl-3-ethylimidazolium chloride, 65039-09-0.

Contribution from the Department of Chemistry,
University of Florence, Florence, Italy

Electronic and CD Spectra of Catecholate and Semiquinonate Adducts of Zinc(II) and Nickel(II) Tetraaza Macrocyclic Complexes

Cristiano Benelli, Andrea Dei,* Dante Gatteschi, and Luca Pardi

Received July 29, 1988

The synthesis, the electrochemical properties, and the electronic and CD spectra of dioxolene adducts of the nickel(II) and zinc(II) complexes with the racemic and the (-)-*SS* isomer of the macrocyclic ligand 5,5,7,12,12,14-hexamethyl-1,4,8,11-tetraazacyclotetradecane, CTH, are reported. The spectra of the catecholate adducts show d-d (nickel) and ligand transitions but no charge transfer. The spectra of the semiquinonate derivatives show a band in the range 11 000-13 000 cm^{-1} that is internal to the ligand and is suggested to be diagnostic of the nature of the dioxolene. A complete assignment is proposed and used to rationalize the relative stability of catecholate and semiquinonate derivatives.

Introduction

In the recent past a significant amount of work has been devoted to the ligand properties of catechol and its oxidation products (semiquinone and quinone) with transition-metal ions.[1-18] The noninnocent character of these ligands has often created ambiguity in assessing the oxidation state of the metal ion. X-ray structural analysis, magnetic measurements, and ESR and vibrational spectroscopy have shown to be powerful tools of investigation. Electronic spectroscopy is not frequently used, the spectra being complicated by the intense absorptions of the dioxolene ligand and by the existence of charge-transfer transitions of different origin. In short, the electronic spectra of the complexes are poorly understood because of the ambiguity in the assignment of the transitions. To date only one work concerning the detailed assignment of the spectra of a series of ruthenium(II)-polypyridine or -bipyridine complexes with variously substituted dioxolene ligands has been reported.[15]

As a part of an effort to explore the electronic properties of molecules containing a paramagnetic metal ion and an organic radical, we have synthesized a number of dioxolene adducts of the type $ML(diox)^{n+}$ (M = Cr, Mn, Fe, Co, Ni, Cu), where diox is a variously substituted dioxolene ligand, either catecholate or semiquinonate, and L is a polyazamacrocyclic ligand.[19] In particular the chemical and physical properties of solid compounds containing the $Ni(CTH)DTBSQ^+$ cation (CTH = *rac*-5,5,7,12,12,14-hexamethyl-1,4,8,11-tetraazacyclotetradecane; DTBSQ = anion of 3,5-di-*tert*-butylbenzo-*o*-semiquinone) have

(1) Pierpont, C. G.; Buchanan, R. M. *Coord. Chem. Rev.* **1981**, *38*, 45.
(2) Kaim, W. *Coord. Chem. Rev.* **1987**, *76*, 187.
(3) Lynch, M. W.; Valentine, M.; Hendrickson, D. N. *J. Am. Chem. Soc.* **1982**, *104*, 6982.
(4) Lynch, M. W.; Hendrickson, D. N.; Fitzgerald, B. R.; Pierpont, C. G. *J. Am. Chem. Soc.* **1981**, *103*, 3961.
(5) Chin, D. H.; Jones, S. E.; Leon, L. E.; Bosserman, P.; Stallings, M. D.; Sawyer, D. T. Biological Redox Components. *ACS Symp. Ser.* **1982**, *No. 201*, 675.
(6) Creber, K. A. M.; Chen, K. S.; Wan, J. K. S. *Rev. Chem. Intermed.* **1984**, *5*, 37.
(7) Kabachnik, M. I.; Bubnov, N. N.; Solodnikov, S. P.; Prokof'ev, A. I. *Russ. Chem. Rev. (Engl. Transl.)* **1984**, *5*, 37.
(8) Cass, M. E.; Gordon, N. R.; Pierpont, C. G. *Inorg. Chem.* **1986**, *25*, 3962.
(9) Buchanan, R. M.; Clafin, J.; Pierpont, C. G. *Inorg. Chem.* **1983**, *22*, 2552.
(10) Kessel, S. L.; Emberson, R. M.; Debrunner, P. G.; Hendrickson, D. N. *Inorg. Chem.* **1980**, *19*, 1170.
(11) Sofen, S. R.; Ware, D. C.; Cooper, S. R.; Raymond, K. N. *Inorg. Chem.* **1979**, *18*, 234.
(12) Stallings, M. D.; Morrison, M. M.; Sawyer, D. T. *Inorg. Chem.* **1981**, *20*, 2655.
(13) Bodini, M. E.; Copia, G.; Robinson, R.; Sawyer, D. T. *Inorg. Chem.* **1983**, *22*, 126.
(14) Lynch, M. W.; Hendrickson, D. N.; Fitzgerald, B. J.; Pierpont, C. G. *J. Am. Chem. Soc.* **1984**, *106*, 2041.
(15) Haga, M.-A.; Dodsworth, E. S.; Lever, A. B. P. *Inorg. Chem.* **1986**, *25*, 447.
(16) Haga, M.-A.; Dodsworth, E. S.; Lever, A. B. P.; Boone, R. S.; Pierpont, C. G. *J. Am. Chem. Soc.* **1986**, *108*, 7413.
(17) Bianchini, C.; Masi, D.; Mealli, C.; Meli, C.; Martini, G.; Laschi, F.; Zanello, P. *Inorg. Chem.* **1987**, *26*, 3683.
(18) Thompson, J. S.; Calabrese, J. C. *Inorg. Chem.* **1985**, *24*, 3167.
(19) Benelli, C.; Dei, A.; Gatteschi, D.; Pardi, L. Manuscript in preparation.

0020-1669/89/1328-1476$01.50/0